

RF Characterization of SiGe HBT Power Amplifiers Under Load Mismatch

Arvind Keerti, *Student Member, IEEE*, and Anh-Vu H. Pham, *Senior Member, IEEE*

Abstract—We present the RF characterization of silicon–germanium heterojunction bipolar transistor (SiGe HBT) power amplifiers (PA) under load mismatched conditions. Experimental results demonstrate a strong dependence of a PA’s RF performance on the phase of mismatched antenna loads. For a load mismatch of voltage standing-wave ratio (VSWR) of 10:1, the 1-dB compressed RF output power ($P_{1\text{ dB}}$), transducer gain (G_T), output third-order intercept point, and power-added efficiency differ by 7.5 dBm, 8.1 dB, 8.3 dBm, and 15%, respectively, between the optimal and worst phase conditions, for an SiGe HBT PA biased at $V_{CC} = 3.3$ V, collector current $I_{CE} = 400$ mA, and frequency of 1.88 GHz. At the optimal phase condition up to VSWR of 10:1, the SiGe HBT PA maintains its linearity, RF output power, gain, and efficiency close to that at a VSWR of 1:1. At all the nonoptimal phases, the deterioration in the RF performance increases with the magnitude of load mismatches. The nonlinear characteristic of a PA under load mismatches is due to amplitude and phase-distortion mechanisms.

Index Terms—Antenna, distortion, linearity, load, mismatch, phase, power amplifier (PA), SiGe HBT, voltage standing-wave ratio (VSWR), wireless.

I. INTRODUCTION

MODERN MOBILE wireless standards like code division multiple access (CDMA)-IS95 and wideband code division multiple access (W-CDMA) use nonconstant envelope modulation schemes, and impose a stringent requirement on the linearity of a power amplifier (PA) in a wireless system. SiGe HBT-based technologies have become a viable solution for high-frequency wireless PAs and transceivers because of their high linearity, high current gain, low noise, and compatibility with BiCMOS processes [1]–[3]. RF linearity characteristics of SiGe HBTs are analyzed in detail using Volterra series [4] and charge control theory [5], whereas the effect of load and source impedances on phase distortion and linearity is analyzed in [6]. The optimization of the input and output matching network for linearity and efficiency in HBT PAs is further discussed in [6]. However, the linearity of SiGe HBT PAs under load mismatches has not been studied.

Manuscript received February 10, 2006; revised August 17, 2006. This work was supported in part by the University of California at Davis and by the University of California MICRO.

A. Keerti was with the Electrical and Computer Engineering Department, University of California at Davis, Davis, CA 95616 USA. He is now with Qualcomm Inc., Campbell, CA 95008 USA (e-mail: akeerti@ece.ucdavis.edu).

A.-V. H. Pham is with the Electrical and Computer Engineering Department, University of California at Davis, Davis, CA 95616 USA (e-mail: pham@ece.ucdavis.edu).

Color versions of one or more of the figures in this paper are available online at <http://ieeexplore.ieee.org>.

Digital Object Identifier 10.1109/TMTT.2006.889326

A wireless device encounters impedance mismatches at the antenna due to signal reflections from the surrounding objects. RF power is reflected back into a PA due to the antenna mismatches and degrades the PA’s linearity, RF output power, and efficiency [7], [8]. Traditionally, an isolator is placed between the PA and an antenna to protect the output power transistor from large voltage/current swings and improve the PA linearity under load mismatches. However, isolators are bulky and expensive for handheld devices, as well as reduce the transmitted power level. Hence, the goal is to develop isolatorless modules for linear PA applications. Previous work on load mismatches has focused on ruggedness of power transistors and control circuitry to protect the transistor at large impedance mismatches [9], [10]. SiGe HBTs are found to be rugged enough to handle large voltage excursions caused by load mismatches [11], [12]. Circuit techniques have been developed to improve the linearity of a PA under antenna mismatches using drive-level adjustment [7], [13]. However, lowering the drive level reduces the output power necessary for a communication link. Tuning circuits are placed between the transceiver and an antenna so that the effective impedance seen towards the antenna at the output of a transmitter is the matched load ($50\ \Omega$), even when the actual antenna impedance is mismatched. These impedance tuners are simple π or T networks with their elements tuned digitally, based on genetic algorithms to achieve high-speed impedance tuning [14]–[17]. In order to maximize the performance of a PA under antenna mismatches, it is imperative to understand the RF output power, linearity, transducer gain, power-added efficiency (PAE), and breakdown voltage of a PA terminated with a mismatched load.

This paper presents a systematic analysis to understand the effect of load impedance mismatches, on RF output power, linearity, transducer gain, PAE, and breakdown voltage of an SiGe HBT PA. At each load voltage standing-wave ratio (VSWR), as the phase of the load reflection coefficient at the output of a PA varies from 0° to 360° , the linearity, RF output power, gain, and efficiency swing from the optimal values to worst values. A performance identical to that of the matched condition is achieved at the optimal phase condition for load mismatches as large as 10:1. At all other phase conditions, the RF performance degrades rapidly. The degradation in the RF performance at the nonoptimal phases increases with a rise in the magnitude of the VSWR. This phase dependence of PA performance under impedance mismatches is pronounced at different collector currents. A detailed investigation shows that the amplitude and phase-distortion mechanisms cause nonlinearities in a PA under load mismatches.

Section II describes the dependence of a PA’s RF parameters on load impedance. Ruggedness of SiGe HBTs is further

TABLE I
REFLECTED POWER AND TRANSMISSION LOSS AT THE ANTENNA

VSWR	Reflected Power (% of transmitted power)	Transmission Loss (dB)
1:1	0.0	0.0
2:1	11.1	0.51
4:1	36.0	1.93
10:1	66.9	4.8

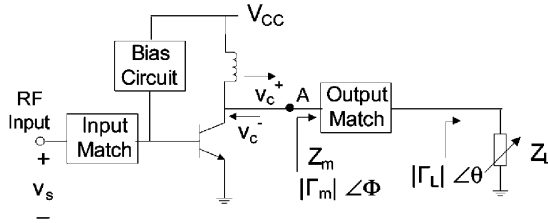


Fig. 1. Block diagram of a PA output stage.

discussed in Section II. Section III shows the measured RF performance of an SiGe HBT PA under load mismatches. Section IV gives detailed analysis to illustrate the cause of RF performance variation and its relation to the load-line impedance. Time-domain analysis is presented to determine the nonlinear mechanism under impedance mismatches. Finally, the measured results of a commercially available SiGe PA under load mismatches are outlined in Section V. In this paper, the term “VSWR” always refers to “load VSWR.”

II. MISMATCH AT ANTENNA

A. Antenna Impedance

The input impedance of an antenna in a wireless communication device is affected by objects in its vicinity. Coupling of an antenna’s radiated field with these surrounding objects changes the antenna input impedance from its nominal value of 50 Ω [18]. This causes an impedance mismatch between an antenna and the transmission line (or matching networks) at its input. Due to this impedance mismatch, RF power is reflected back into a transmitter. As shown in Table I, the reflected power is as high as 36% of the transmitted power and the transmission loss through an antenna is ~ 2 dB when its input impedance is mismatched by a magnitude of VSWR of 4:1.

B. PA Performance

A PA is the key component determining the linearity, efficiency, and power transmitted from the transmitter chain. Due to antenna mismatches, the reflected power flows back directly into a PA and affects its performance more significantly than the losses in the antenna itself. Fig. 1 shows the output stage of a PA connected to the load (antenna) Z_L . When the load impedance (or load reflection coefficient Γ_L) alters, the effective impedance Z_m (and reflection coefficient Γ_m) seen by the collector of a transistor is changed by

$$Z_m = Z_{11} - \frac{Z_{12}^2}{Z_{22} + Z_L} \quad (1)$$

where $[Z]$ is the Z -parameters of the PA output matching network, which is passive and reciprocal.

The load line of a transistor changes depending on the magnitude and phase of reflection coefficient Γ_m at the collector [7]. Thus, the SiGe HBT is no longer terminated by the optimum load-line matched impedance (Z_{mopt}) required to achieve optimal RF performance—maximum output power, PAE, and linearity [19].

C. SiGe HBT Breakdown Voltage

Ruggedness of a transistor is a concern in PAs since large voltages appear at the collector under load mismatches and can result in damage to the HBTs. The maximum peak collector voltage is expressed as

$$V_{cmax} = V_{CC} + |v_c^+| |1 + |\Gamma_m| e^{j\phi}| \quad (2)$$

where V_{CC} is the dc-bias voltage.

At high collector voltages, the electric field is high and avalanche breakdown occurs when the base current becomes negative [20]. If the impedance of a bias circuit driving the RF transistor is high (a current source applied at the base), the collector–base breakdown current is fed back into the base–emitter junction and the base–emitter voltage increases. The collector current increases and breakdown occurs due to thermal runaway. This occurs at the conventional BV_{CEO} . If the impedance of a bias circuit driving the RF transistor is low (a voltage source applied at the base), the collector–base breakdown current is initially shunted by the external base biasing resistor and breakdown occurs at a voltage higher than the BV_{CEO} [12].

In linear SiGe HBT PAs, dc bias is usually applied through high-impedance current mirror circuit and, hence, the bias voltage should not exceed the BV_{CEO} . However, these transistors are driven by low-impedance networks and, thus, peak RF voltage swings well above BV_{CEO} , close to BV_{CBO} [11]. The work in [11] demonstrated that the relevant breakdown voltage for an SiGe HBT in a 0.5- μm SiGe BiCMOS process (similar to the one used for this work) is the voltage under emitter open breakdown (BV_{CBO}) or base grounded breakdown (BV_{CER}) condition instead of the conventional lower open circuit condition of V_{CEO} .

III. SiGe HBT PA—RESULTS AND DISCUSSION

A. Measurement Setup

On-wafer load–pull measurements are performed on an SiGe HBT of emitter area (A_E) = 1960 μm^2 fabricated in an IBM 0.5- μm SiGe BiCMOS process. Fig. 2 shows the transistor formed by connecting 96 unit cells ($0.5 \mu\text{m} \times 20 \mu\text{m} \times 2$) in parallel. A ballasting resistor of 3.86 Ω is added in the emitter of each unit cell for thermal stability.

The Maury Microwave automatic tuner system (ATS) used for on-wafer load–pull measurements is shown in Fig. 3. It consists of an SiGe HBT as the device-under-test (DUT), a tuner at the output (T2), and a tuner at the input (T1). The DUT is placed on a Cascade Microwave probe station. The input and output fixtures consist of low-loss 150- μm -pitch microwave

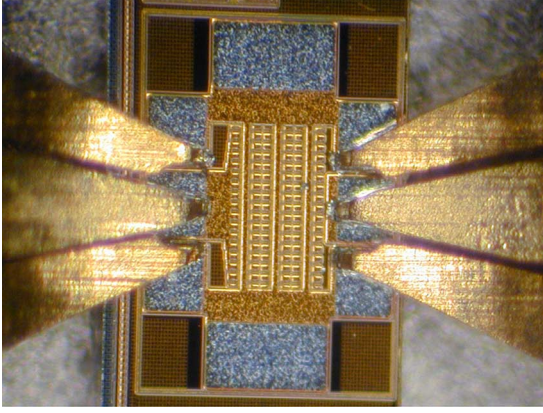


Fig. 2. Fabricated IBM SiGe HBT.

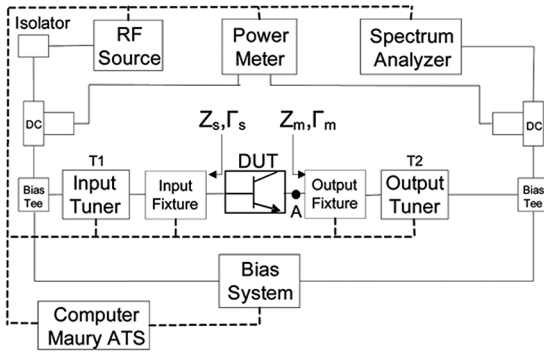


Fig. 3. Load-pull measurement setup for load mismatches.

probes and cables. Initially, the output fixture with the output tuner T2 (tuned for maximum output power) serves as the output matching network, and the input fixture with the input tuner T1 (tuned for maximum gain) serves as the input matching network, thereby constituting a PA. The load impedance Z_L at the output of tuner T2 is 50Ω . For mismatch measurements, the ATS software automatically determines the effective impedance Z_m by emulating the load impedance Z_L variations (assuming the output matching network is fixed). This effective impedance Z_m is due to the cascaded combination of the output matching network and the load. Consequently, the output tuner T2 is directly tuned to synthesize the effective impedance Z_m , as seen by the output of a DUT under varying load impedances. During mismatch measurements, the output fixture and tuner T2 represent the cascaded combination of the output matching network and the load.

Thus, load is varied to change the magnitude and phase of Γ_L and to create a specific impedance mismatch for this study. The measured S -parameters of each block (tuners, fixtures, directional couplers, bias tees, and isolators) in the load-pull system are incorporated into the computer-controlled ATS software and SiGe HBT is deembedded to set the reference planes at the collector and base of a transistor. This facilitates the measurement of the RF power at node A (collector of transistor). A constant current (base current I_b) bias is applied to the base of an SiGe HBT through a resistive type constant current source and input bias tee, while the collector is biased at a supply voltage of 3.3 V through an output bias tee.

TABLE II
LOAD-LINE MATCHED IMPEDANCE

I_{CE} (mA)	Z_{mopt} (Ω)
400	$4.88 - j * .034$
200	$4.91 + j * 1.5$
100	$6.77 + j * 5.9$
20	$5.41 + j * 3.27$

TABLE III
SiGe HBT PA PERFORMANCE AT $Z_L = 50 \Omega$

Parameters	Units	SiGe HBT PA
P_{1dB}	dBm	23.7
OIP3	dBm	34.6
G_T	dB	14.5
PAE	%	18.32

An SiGe HBT, biased at $I_{CE} = 400$ mA, is matched at the output to $Z_{mopt} = (4.88 - j * 0.34) \Omega$ to achieve a maximum RF output power and at the input to $Z_s = (3.4 - j * 0.1) \Omega$ to achieve a maximum transducer gain. This constitutes an SiGe HBT PA whose load Z_L is initially set to a $50\text{-}\Omega$ matched condition. Two-tone measurements are conducted to determine the fundamental and third-order intermodulation component of the RF output power at the output of a transistor (node A). Further, the load is tuned for $|\Gamma_L| = 0.6$ (VSWR = 4 : 1) and $|\Gamma_L| = 0.818$ (VSWR = 10 : 1), respectively, and two-tone measurements are carried out at phases (θ) of these $|\Gamma_L|$ in steps of 30° . RF performance of this discrete SiGe HBT PA is measured for all the above-mentioned load conditions at a frequency $f = 1.88$ GHz, a supply voltage $V_{CC} = 3.3$ V, and collector bias currents $I_{CE} = 400, 200, 100,$ and 20 mA, respectively. Impedance Z_s is same for all the collector currents and the source tuner is fixed for all measurements. Impedance $Z_{mopt}(\Gamma_{mopt})$ changes with collector currents and the output tuner is tuned for each I_{CE} . Table II shows the optimum load-line matched impedance Z_{mopt} for different collector currents.

B. RF Performance— $V_{CC} = 3.3$ V, $I_{CE} = 400$ mA

Table III summarizes the measured RF performance of an SiGe HBT PA, at $50\text{-}\Omega$ load (Z_L), $f = 1.88$ GHz, in class A mode with $V_{CC} = 3.3$ V, and $I_{CE} = 400$ mA. The PAE is reported at P_{1dB} , while G_T is the maximum value. RF output power at $50\text{-}\Omega$ load termination is slightly lower than other reported devices [21] due to a small series resistance at the base resulting in lower effective beta.

The RF performance of an SiGe HBT PA, measured at $f = 1.88$ GHz, $V_{CC} = 3.3$ V, $I_{CE} = 400$ mA, and a load (Z_L) mismatch magnitude of VSWR = 10 : 1 is shown in Fig. 4. As seen from this figure, the P_{1dB} , G_T , PAE, and output third-order intercept point (OIP3) vary with the phase (θ) of the load reflection coefficient. The optimal P_{1dB} , OIP3, G_T , and PAE occur at $\theta = 180^\circ$, which is referred as the optimal phase condition. The worst degradation in P_{1dB} , OIP3, G_T , and PAE occurs at $\theta = 0^\circ$, which is referred as the worst phase condition. P_{1dB} swings from 23.5 to 16 dBm, OIP3 varies from 34.9

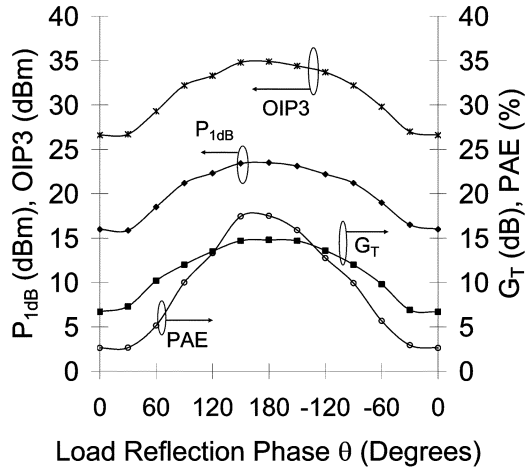


Fig. 4. Measured RF output power ($P_{1\text{ dB}}$), OIP3, G_T , and PAE of an SiGe HBT PA at VSWR = 10 : 1, $f = 1.88\text{ GHz}$, $V_{CC} = 3.3\text{ V}$, $I_{CE} = 400\text{ mA}$.

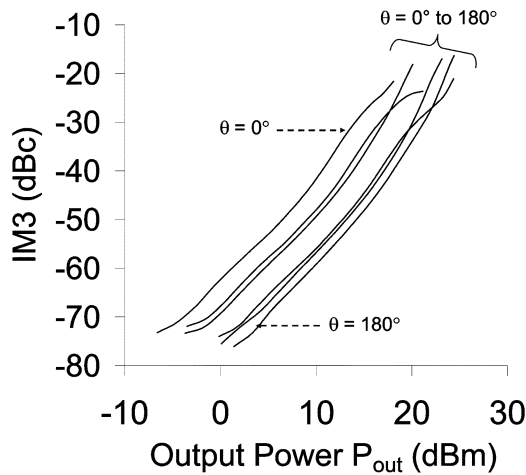


Fig. 5. Measured IM3 of an SiGe HBT PA at VSWR = 10 : 1, $f = 1.88\text{ GHz}$, $V_{CC} = 3.3\text{ V}$, $I_{CE} = 400\text{ mA}$.

to 26.6 dBm, G_T varies from 14.8 to 6.7 dB, while the PAE changes from 17.5% to 2.63%.

The third-order intermodulation (IM3) distortion ratio over the RF output power at VSWR = 10 : 1 for the same bias condition is shown in Fig. 5. IM3 varies with θ for all the output power levels. Highest IM3 occurs at $\theta = 0^\circ$ and lowest at $\theta = 180^\circ$, where linearity is the best. IM3 differs by $\sim 18\text{ dBc}$ between the optimal and worst phase conditions at VSWR = 10 : 1 for output power levels up to 20 dBm.

Fig. 6 shows the measured RF output power ($P_{1\text{ dB}}$), transducer gain, PAE, and OIP3 of an SiGe HBT PA with varying VSWR at the worst phase condition and the optimal phase condition, respectively. At the nonoptimal phases of Γ_L , the RF output power ($P_{1\text{ dB}}$), transducer gain, PAE, and OIP3 drop rapidly as the magnitude of Γ_L increases. However, at the optimal phase condition, these four performance parameters have values close to that of the 50- Ω load termination. Define $\Delta\text{OIP3} = \text{OIP3}(\text{optimal phase}) - \text{OIP3}(\text{worst phase})$; $\Delta P_{1\text{ dB}} = P_{1\text{ dB}}(\text{optimal phase}) - P_{1\text{ dB}}(\text{worst phase})$; $\Delta G_T = G_T(\text{optimal phase}) - G_T(\text{worst phase})$;

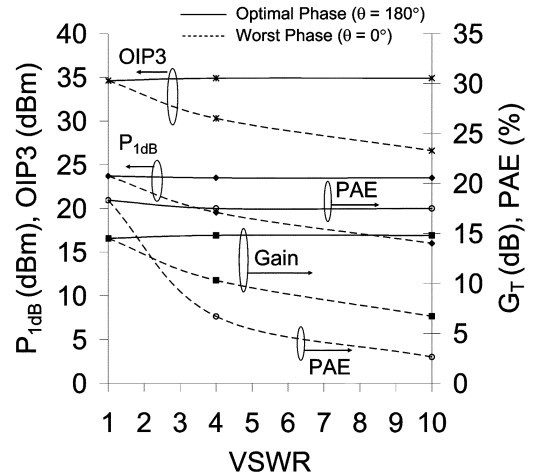


Fig. 6. Measured RF output power ($P_{1\text{ dB}}$), OIP3, G_T , and PAE of an SiGe HBT PA with magnitude of load mismatch, at optimal ($\theta = 180^\circ$), and worst ($\theta = 0^\circ$) phases, $f = 1.88\text{ GHz}$, $V_{CC} = 3.3\text{ V}$, $I_{CE} = 400\text{ mA}$.

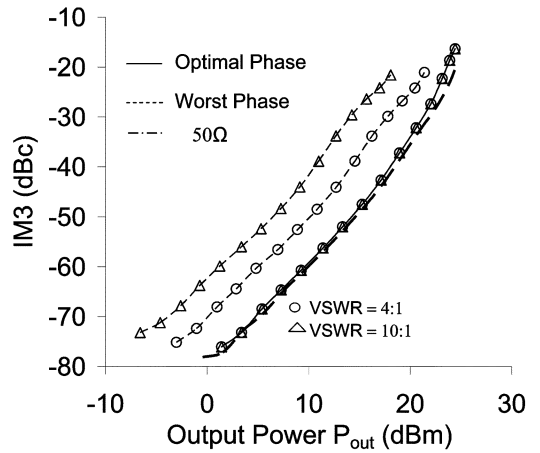


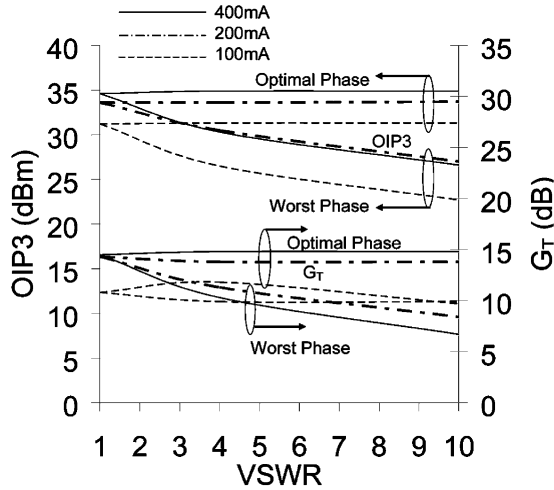
Fig. 7. Measured IM3 of an SiGe HBT PA at different VSWRs, at optimal ($\theta = 180^\circ$), and worst ($\theta = 0^\circ$) phases, $f = 1.88\text{ GHz}$, $V_{CC} = 3.3\text{ V}$, $I_{CE} = 400\text{ mA}$.

$\Delta\text{PAE} = \text{PAE}(\text{optimal phase}) - \text{PAE}(\text{worst phase})$. ΔOIP3 , $\Delta P_{1\text{ dB}}$, ΔG_T , and ΔPAE increase as VSWR rises.

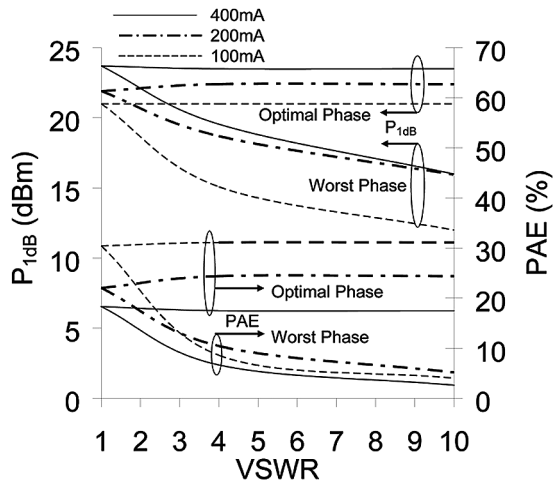
IM3 over the RF output power for different VSWRs, at the optimal and worst phase condition, is shown in Fig. 7. For all the output power levels, the IM3 increases with $|\Gamma_L|$ at all the phases of Γ_L other than the optimal phase, where it is close to the 50- Ω matched condition.

C. RF Performance as Function of I_{CE}

The RF performance of an SiGe HBT PA as a function of I_{CE} is shown in Fig. 8(a) and (b). Under load mismatches, RF performance of a PA at each I_{CE} varies with phases of load reflection coefficient, similar to the class A bias condition ($I_{CE} = 400\text{ mA}$). The optimum performance and the worst degradation occur at $\theta = 150^\circ$ and $\theta = -30^\circ$, respectively, for $I_{CE} = 200, 100,$ and 20 mA , as compared to $\theta = 180^\circ$ and $\theta = 0^\circ$, respectively, for $I_{CE} = 400\text{ mA}$. This is because the optimum load-line matched impedance $Z_{m\text{opt}}$ changes with collector currents, becoming more inductive as I_{CE} is decreased. As collector current varies from $I_{CE} = 400\text{ mA}$



(a)



(b)

Fig. 8. (a) Measured OIP3 and G_T of an SiGe HBT PA with magnitude of mismatch as a function of I_{CE} at $f = 1.88$ GHz, $V_{CC} = 3.3$ V. (b) Measured $P_{1\text{dB}}$ and PAE of an SiGe HBT PA with magnitude of mismatch as a function of I_{CE} at $f = 1.88$ GHz, $V_{CC} = 3.3$ V.

to $I_{CE} = 100$ mA, ΔPAE increases from 14.5% to 27.5%, whereas ΔG_T decreases by ~ 8 dB at a load VSWR of 10 : 1. $\Delta P_{1\text{dB}}$ and ΔOIP3 decrease by ~ 1 and 1.6 dBm, respectively, as I_{CE} changes from 400 to 200 mA at the same load VSWR. However, as I_{CE} is decreased from 200 to 100 mA, both $\Delta P_{1\text{dB}}$ and ΔOIP3 increase by ~ 2.5 dBm.

Fig. 9 shows the IM3 distortion ratio with varying I_{CE} at VSWR = 10 : 1 for an SiGe HBT PA. It is seen that the absolute value of IM3 decreases with increase in I_{CE} for all the phases of Γ_L at all the RF output power levels. Difference between the optimal and worst phase IM3 is ~ 18 dBc for $I_{CE} = 400$ mA, and this difference further decreases with decrease in I_{CE} , exhibiting a smaller difference at $I_{CE} = 20$ mA. As the collector current reduces, the SiGe HBT approaches towards class B mode, where it is highly nonlinear and the effect of terminating load impedance on linearity is less as compared to that at higher collector currents

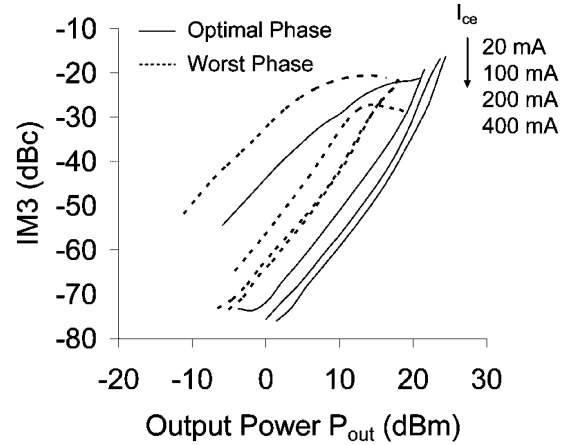


Fig. 9. Measured IM3 of an SiGe HBT PA as a function of I_{CE} at VSWR = 10 : 1, optimal and worst phases, $f = 1.88$ GHz, $V_{CC} = 3.3$ V.

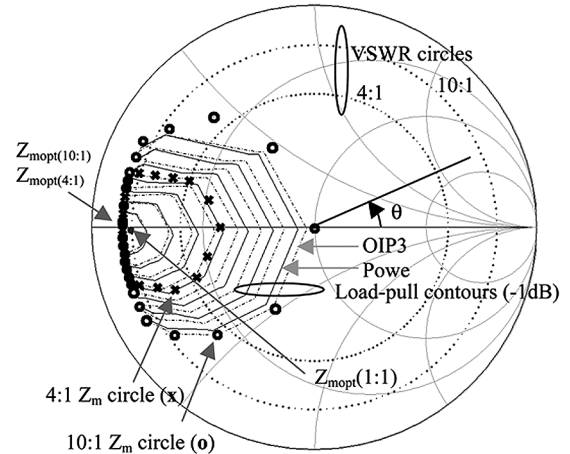


Fig. 10. Smith chart showing load-pull contours, and the VSWR circles and Z_m circles for an SiGe HBT PA at load mismatches of VSWR = 4 : 1, 10 : 1, and all phases.

Finally, during measurements, the SiGe HBT did not break down and survived load mismatches up to VSWR = 10 : 1, as evident from the work in [11].

IV. PERFORMANCE ANALYSIS

Measurement results in Section III demonstrate the effect of load mismatches on the RF performance of an SiGe HBT PA. System-level analysis is provided here to understand the effect of load changes on the PA's RF output power, transducer gain, PAE, and linearity. Further, time-domain analysis is used to investigate the linearity behavior under load mismatches.

A. Load-Line Impedance and Load-Pull Contours

The measured impedance Z_m seen by the collector of a transistor under matched and mismatched load is plotted on a Smith chart in Fig. 10. Fig. 10 shows the load-pull contours, Z_m circles, and VSWR circles. The load-pull contours for RF output power and OIP3 are shown in Fig. 10, whereas G_T and the PAE contours closely overlap with the power contours. $Z_{m\text{opt}(1:1)} = (4.88 - j * 0.34) \Omega$ is the load-line matched impedance, determined through load-pull measurements, for an SiGe HBT ($I_{CE} = 400$ mA, $V_{CC} = 3.3$ V) under a

matched 50- Ω load. This impedance point is the center of the oval-shaped load–pull contours, and the power (or OIP3) drops by 1 dBm for each contour from its center. As the normalized load reflection coefficient Γ_L is varied through all the phase angles at VSWR of 4:1 and 10:1 (shown by VSWR circles at the center), the corresponding transformed impedance Z_m is represented by the smaller circles towards the left of the Smith chart. The inner smaller circle (denoted by \times) represents Z_m at VSWR of 4:1 and outer smaller circle (denoted by \circ) represents Z_m at VSWR of 10:1, for all values of θ . At the center of the smaller circles is $Z_{mopt(1:1)}$. It is seen that since $Z_{mopt(1:1)}$ is a small value, the Z_m circles compress towards the left edge of the Smith chart occupying a smaller area.

It is observed from the load–pull power measurements that there is a Z_{mopt} on each Z_m circle, which corresponds to the optimal phase condition. $Z_{mopt(4:1)} = (3.77 - j * 0.28) \Omega$ is the Z_{mopt} for the VSWR of 4:1. $Z_{mopt(10:1)}$ for the VSWR of 10:1 also occurs at the same point in this case. As seen from Fig. 10, $Z_{mopt(4:1)}$ and $Z_{mopt(10:1)}$ are very close to $Z_{mopt(1:1)}$ and, hence, the SiGe HBT is capable of delivering the RF output power ($P_{1\text{ dB}}$), transducer gain, PAE, and OIP3 corresponding to that of the 50- Ω case at all the Z_{mopt} impedance points up to a VSWR of 10:1.

For each Z_m circle, at all other Z_m values (or phases of Γ_L) other than its Z_{mopt} , the RF output power ($P_{1\text{ dB}}$), OIP3, gain, and PAE degrade as Z_m moves away from its Z_{mopt} . The worst degradation in the RF performance for the SiGe HBT PA occurs at impedances $(20.4 + j * 2.3) \Omega$ and $(50.14 + j * 0.0) \Omega$ for a VSWR of 4:1 and 10:1, respectively. As evident from the Z_m contours in Fig. 10, these impedances points are the farthest (at 180° offset) from its Z_{mopt} , and collector voltage swing at these points is high. Hence, the power drop at these points is the maximum. For larger magnitudes of Γ_L , the Z_m circles are spread out, as seen for VSWR = 10 : 1 in Fig. 10. As a result, the impedance Z_m at the nonoptimal phases of Γ_L moves further away from its Z_{mopt} on each Z_m circle and collector voltage excursions are still larger. This causes the increasing drop in RF output power ($P_{1\text{ dB}}$), OIP3, gain, and PAE with an increase in the magnitude of load mismatch.

Z_m depends on the phase shift through the output matching network and the load Z_L , as determined through (1). Since the elements of the output matching network (or output tuner) are fixed, the phase of Γ_L at which $Z_m = Z_{mopt}$ is the same for each load VSWR. In this case, Z_{mopt} occurs at $\theta = 180^\circ$ for each load VSWR and the RF performance is optimum at this phase of Γ_L for all load VSWRs. Similarly, the worst degradation occurs at the same phase of Γ_L for each load VSWR. As the collector current decreases, $Z_{mopt(1:1)}$ becomes inductive and the load–pull contours are oriented at an axial symmetry along 150° (–30°) phase of Γ_L . Hence, the optimal performance is at a load reflection phase of $\theta = 150^\circ$ and the worst degradation is at $\theta = -30^\circ$.

Impedance Z_m depends on the output matching network of a PA, and the varying load impedance. For a PA, the output matching network is not unique and it may vary from one implementation to another. If the output matching network is changed, then the phase of the load reflection coefficient at which RF performance is optimum (or worst) is relatively

shifted depending on the phase shift through a matching network.

B. Linearity

Time-domain analysis is performed to further analyze the linearity phenomena of an SiGe HBT PA under load mismatches. The nonlinear characteristics in a PA produce amplitude and phase distortions. If the RF input power is large, the SiGe HBT saturates and causes voltage clipping at positive and negative peaks of the modulated output waveform. This results in amplitude modulation to amplitude modulation (AM–AM) distortion—compression of the transfer characteristic as the drive level is increased. Amplitude modulation to phase modulation (AM–PM) is the change in phase of the transfer characteristic as the drive level is increased [22]. Consider a two-tone envelope signal applied to the input of an SiGe HBT given by

$$v_s(t) = v \cos(\omega_1 t) + v \cos(\omega_2 t). \quad (3)$$

The RF output voltage at the collector is distorted and is represented as [19]

$$v_c(t) = A \cos(\omega_m t) \cos \left[\omega t + \frac{\phi}{2} (1 + \cos(2\omega_m t)) \right]$$

where

$$\begin{aligned} \omega_m &= \frac{\omega_1 - \omega_2}{2} \\ \omega &= \frac{\omega_1 + \omega_2}{2}. \end{aligned} \quad (4)$$

A is the peak voltage amplitude of output envelope signal. ϕ is the peak magnitude of the AM–PM phase shift occurring at the positive or negative amplitude peaks of the modulated output voltage waveform [19]. ϕ is assumed to be small, and $\phi \ll 1$ radians. This phase shift depends on the nonlinear output and base–collector capacitance of an HBT and the matching impedance Z_m at the collector. Analysis in [6] shows the strong dependence of the phase shift ϕ on the impedance Z_m .

The magnitude of each of the fundamental components, and the magnitude of each of the IM3 components of RF output voltage at the collector of an SiGe HBT are represented by (5) and (6), respectively, as follows:

$$v_{cfund} = A \left(\frac{\mu_1}{2} \cos \left[(\omega \pm \omega_m) t - \frac{\phi}{2} \right] + \frac{\phi}{8} \sin(\omega \pm \omega_m) t \right) \quad (5)$$

$$v_{cim3} = \left(\frac{\mu_3}{2} \cos \left[(\omega \pm 3\omega_m) t - \frac{\phi}{2} \right] + \frac{\phi}{8} \sin(\omega \pm 3\omega_m) t \right) t \quad (6)$$

where μ_1 and μ_3 are the first- and third-order distortion terms due to AM–AM nonlinearities. The phase shift ϕ is the contribution from the AM–PM distortion. Thus, the amplitude and phase distortion affects the IM3 products significantly and increases the IM3 levels. It is difficult to measure the individual contributions of the two distortion phenomena to the IM3. Hence, the phase distortion at output of a PA is plotted to illustrate that the AM–PM is contributing to the nonlinearities under load mismatches up to VSWR = 10 : 1. Fig. 11 shows the mea-

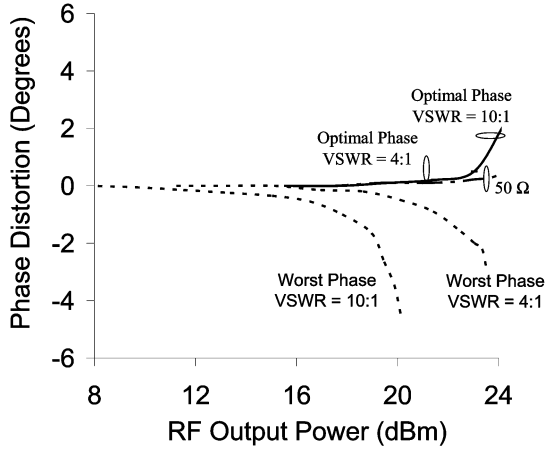


Fig. 11. Measured phase distortion of an SiGe HBT PA at 50 Ω , optimal ($\theta = 180^\circ$) and worst ($\theta = 0^\circ$) phases at VSWR of 4:1 and 10:1, $f = 1.88$ GHz, $V_{CC} = 3.3$ V, $I_{CE} = 400$ mA.

sured phase distortion at the output of an SiGe HBT PA as a function of the RF output power for the 50- Ω load condition, and the optimal and worst phase conditions at a load VSWR of 4:1 and 10:1, respectively. At the optimal phase condition up to VSWR = 10 : 1, the phase distortion is almost zero at $P_{out} = 23$ dBm, but at the worst phase condition, there is a significant amount of phase distortion of 3° at $P_{out} = 23$ dBm for VSWR = 4 : 1 and further increases as seen for VSWR = 10 : 1. The phase distortion is dominant at all other phases of Γ_L , except at the optimal phase. This causes a reduction in fundamental RF output power and an increase in IM3 levels over the phase of Γ_L . Thus, time-domain analysis quantifies that the degradation in linearity under load mismatches is due to amplitude (voltage clipping), as well as phase distortion.

V. WIRELESS PA—RESULTS

The effect of load mismatches is experimentally demonstrated on a commercially available SiGe PA circuit at frequency $f = 2.4$ GHz and $V_{CC} = 3.3$ V. Input and output matching networks are a part of this PA circuit, and a tuner (T2) is used only to vary the load impedance. RF performance is measured at the load Z_L , rather than at the collector as in the previous sections. SiGe PA at a frequency of 2.4 GHz and 3.3-V supply voltage has similar characteristics at VSWR = 10 : 1 with the $P_{1\text{dB}}$ varying from 18 to 13 dBm; OIP3 swinging from 29 to 22.3 dBm, and G_T varies by 4 dB. Fig. 12 shows the measured RF output power ($P_{1\text{dB}}$), transducer gain, PAE, and OIP3 of the PA with varying VSWR (magnitude of Γ_L) at the worst phase condition and the optimal phase condition, respectively. The optimal performance occurs at $\theta = 150^\circ$, and the worst degradation occurs at $\theta = -30^\circ$ due to a different matching network than the one used in Section III. As the magnitude of load mismatch increases, the RF output power ($P_{1\text{dB}}$), OIP3, and G_T at the worst phase condition decreases for the PA. However, at the optimal phase condition, the RF output power ($P_{1\text{dB}}$), OIP3, and G_T remains close to that of the 50- Ω condition up to a VSWR of 6:1. PAE reduces drastically with impedance mismatch at all the phases. This experiment on the PA circuit illustrates that the PA circuit's response to

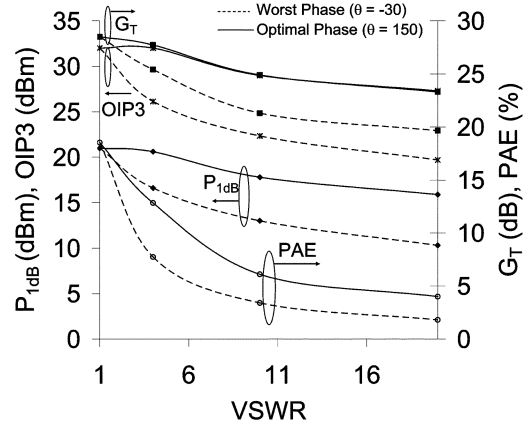


Fig. 12. Measured RF output power ($P_{1\text{dB}}$), OIP3, G_T , and PAE of an SiGe PA with magnitude of mismatch, optimal ($\theta = 150^\circ$), and worst ($\theta = -30^\circ$) phases, $f = 2.4$ GHz, $V_{CC} = 3.3$ V.

load mismatches is analogous to that of a hybrid SiGe HBT PA analyzed in Section IV. The only small deviation is in the PAE performance. The optimum $Z_{mopt(1:1)}$ selected for an SiGe HBT used in the PA circuit, and the matching network, are the possible causes of the minor deviation in PAE performance.

VI. CONCLUSION

Characterization of an SiGe HBT PA under load mismatches empowers the development of circuit techniques to improve the PA RF performance, and provides insight for isolatorless linear PA modules. It has been found that the RF output power, linearity, efficiency, and transducer gain of an SiGe HBT PA is heavily dependent on the phase of load. RF performance of a PA under severe impedance mismatches (up to VSWR of 10:1) stays close to that at 50 Ω , at an optimum phase of load reflection coefficient, whereas it degrades at all other phases. The deterioration in the RF performance at the nonoptimal phases increases with a rise in the magnitude of load VSWR. Time-domain analysis demonstrates that the AM-AM and AM-PM distortion mechanisms cause linearity degradation under load mismatches.

ACKNOWLEDGMENT

The authors would like to thank Dr. P. Zampardi, Skyworks Solutions Inc., Newbury Park, CA, for reviewing this study and providing his valuable suggestions. The authors also acknowledge Tahoe RF Semiconductor Inc., Auburn, CA, and IBM Inc., Yorktown Heights, NY, for support and fabrication.

REFERENCES

- [1] J. D. Cressler, "SiGe HBT technology: A new contender for Si-based RF and microwave circuit applications," *IEEE Trans. Microw. Theory Tech.*, vol. 46, no. 5, pp. 572–589, May 1998.
- [2] A. Raghavan, D. Heo, M. Maeng, A. Sutono, K. Lim, and J. Laskar, "A 2.4 GHz high efficiency SiGe HBT power amplifier with high-Q LTCC harmonic suppression filter," in *IEEE MTT-S Int. Microw. Symp. Dig.*, Seattle, WA, Jun. 2002, vol. 2, pp. 1019–1022.
- [3] P. D. Tseng, L. Zhang, G.-B. Gao, and M. F. Chang, "A 3-V monolithic SiGe HBT power amplifier for dual-mode (CDMA/AMS) cellular handset applications," *IEEE J. Solid-State Circuits*, vol. 35, no. 9, pp. 1338–1344, Sep. 2000.

- [4] G. Niu, Q. Liang, J. D. Cressler, C. S. Webster, and D. L. Harnam, "RF linearity characteristics of SiGe HBTs," *IEEE Trans. Microw. Theory Tech.*, vol. 49, no. 9, pp. 1558–1565, Sep. 2001.
- [5] M. Vaidyanathan, M. Iwamoto, L. E. Larson, P. S. Gudem, and P. M. Asbeck, "A theory of high-frequency distortion in bipolar transistors," *IEEE Trans. Microw. Theory Tech.*, vol. 51, no. 2, pp. 448–461, Feb. 2003.
- [6] T. Iwai, S. Ohara, H. Yamada, Y. Yamaguchi, K. Imanishi, and K. Joshin, "High efficiency and high linearity InGaP/GaAs HBT power amplifiers: Matching techniques of source and load impedance to improve phase distortion and linearity," *IEEE Trans. Electron Devices*, vol. 45, no. 6, pp. 1196–1200, Jun. 1998.
- [7] A. van Bezooijen, C. Chanlo, and A. H. M. van Roermund, "Adaptively preserving power amplifier linearity under antenna mismatch," in *IEEE MTT-S Int. Microw. Symp. Dig.*, Philadelphia, PA, Jun. 2003, vol. 3, pp. 1515–1518.
- [8] A. Keerti and A. Pham, "Dynamic output phase to adaptively improve the linearity of the power amplifier under antenna mismatch," in *IEEE Radio Freq. Integr. Circuits Symp.*, Long Beach, CA, Jun. 2005, pp. 675–678.
- [9] J. Pusi, S. Sridharan, P. Antognetti, D. Helms, A. Nigam, J. Griffiths, K. Louie, and M. Doherty, "SiGe power amplifiers ICs with VSWR protection for handset applications," *Microw. J.*, pp. 100–113, Jun. 2001.
- [10] M. Spirito, L. C. N. de Vreede, L. K. Nanver, S. Weber, and J. N. Burghartz, "Power amplifier PAE and ruggedness optimization by second harmonic control," *IEEE J. Solid-State Circuits*, vol. 38, no. 9, pp. 1575–1583, Sep. 2003.
- [11] J. B. Johnson, A. J. Joseph, D. C. Sheridan, R. M. Maladi, P. O. Brandt, J. Persson, J. Andersson, A. Bjorneklett, U. Persson, F. Abasi, and L. Tilly, "Silicon-germanium BiCMOS HBT technology for wireless power amplifier applications," *IEEE J. Solid-State Circuits*, vol. 39, no. 10, pp. 1605–1614, Oct. 2004.
- [12] A. Inoue, S. Nakatsuka, R. Hattori, and Y. Matsuda, "The maximum operating region in SiGe HBT's for RF power amplifiers," in *IEEE MTT-S Int. Microw. Symp. Dig.*, Seattle, WA, Jun. 2002, pp. 1023–1026.
- [13] K. Yamamoto, S. Suzuki, K. Mori, T. Asada, T. Okuda, A. Inoue, T. Miura, K. Chomei, R. Hattori, M. Yamanouchi, and T. Shimura, "A 3.2-V operation single-chip dual-band AlGaAs/GaAs HBT MMIC power amplifier with active feedback circuit technique," *IEEE J. Solid-State Circuits*, vol. 35, no. 8, pp. 1109–1120, Aug. 2000.
- [14] Y. Sun and J. K. Fidler, "High speed automatic antenna tuning units," in *9th Int. Antennas Propag. Conf.*, Eindhoven, The Netherlands, Apr. 1995, vol. 1, pp. 218–222.
- [15] M. Thompson and J. K. Fidler, "Fast antenna tuning using transponder based simulation annealing," *Electron. Lett.*, vol. 36, no. 7, pp. 603–604, Mar. 2000.
- [16] J. J. Mallorqui, A. Aguias, A. Cardama, R. Pagés, and J. M. Haro, "Automatic self-matching network for industrial microwave heating base don conjugate gradient algorithm," *Electron. Lett.*, vol. 35, no. 4, pp. 311–312, Feb. 1999.
- [17] J. de Mingo, A. Crespo, A. Valdovinos, D. Navarro, and P. García, "A radio frequency electronically controlled impedance tuning network design and its application to antenna input impedance automatic matching system," *IEEE Trans. Microw. Theory Tech.*, vol. 52, no. 2, pp. 489–497, Feb. 2004.
- [18] S. R. Best, "Antenna properties and their impact on wireless system performance," Cushcraft Corporation, Manchester, NH, 1998 [Online]. Available: <http://www.cushcraft.com/comm/support/pdf/Antenna-Properties-an-14998.pdf>
- [19] S. Cripps, *RF Power Amplifiers for Wireless Communications*. Norwood, MA: Artech House, 1999.
- [20] S. Heckmann, R. Sommet, J. M. Nebus, J. C. Jacquet, D. Floriot, P. Auxemery, and R. Quere, "Characterization and modeling of bias dependent breakdown and self-heating in GaInP/GaAs power HBT to improve high power amplifier design," *IEEE Trans. Microw. Theory Tech.*, vol. 50, no. 12, pp. 2811–2819, Dec. 2002.
- [21] J. Deng, P. S. Gudem, L. E. Larson, and P. M. Asbeck, "A high average-efficiency SiGe HBT power amplifier for WCDMA handset applications," *IEEE Trans. Microw. Theory Tech.*, vol. 53, no. 2, pp. 529–537, Feb. 2005.
- [22] P. B. Kenington, *High-Linearity RF Amplifier Design*. Norwood, MA: Artech House, 2000.



Arvind Keerti (S'05) received the B.E. degree in electronics engineering from the University of Pune, Pune, India, in 1999, and the M.S. and Ph.D. degrees in electrical engineering from the University of California at Davis, in 2004 and 2006, respectively.

From 2000 to 2001, he was a Design Engineer with Motorola Inc., Noida, India, where he developed application-specific integrated circuits (ASICs) for cellular handsets. He is currently an RF Integrated Circuit (RFIC) Design Engineer with Qualcomm Inc., Campbell, CA. His research interests are RFICs for

wireless communication systems.



Anh-Vu H. Pham (SM'03) received the B.E.E. (with highest honors), M.S., and Ph.D. degrees from the Georgia Institute of Technology, Atlanta, in 1995, 1997, and 1999, respectively.

In 1997, he cofounded RF Solutions LLC, an RFIC company that was acquired by Anadigics in 2003. He has held faculty positions with Clemson University and the University of California at Davis, where he is currently an Associate Professor. He is also active as a consultant to industry. He coauthored approximately 60 technical papers. His research inter-

ests are in the area of RF and high-speed packaging and signal integrity and RFIC design.

Dr. Pham is a member of the IEEE Microwave Theory and Techniques Society (IEEE MTT-S) International Microwave Symposium (IMS) Technical Program Committee (TPC) on Power Amplifiers and Integrated Circuits. He has been the chair of the IEEE MTT-12 Microwave and Millimeter Wave Packaging and Manufacturing Technical Committee of the IEEE MTT-S. He was the recipient of the 2001 National Science Foundation CAREER Award.